Available online at www.sciencedirect.com

SCIENCE DIRECT®

Coastal Engineering 52 (2005) 1–23

Coastal Engineering
An International Journal for Coastal, Harbour and Offshore Engineers

www.elsevier.com/locate/coastaleng

On the transport of suspended sediment by a swash event on a plane beach

David Pritchard[a,*], Andrew J. Hogg[b]

[a]BP Institute for Multiphase Flow, University of Cambridge, Madingley Rise, Cambridge CB3 0EZ, England, United Kingdom
[b]Centre for Environmental and Geophysical Flows, School of Mathematics, University of Bristol, University Walk, Bristol BS8 1TW, England, United Kingdom

Received 5 April 2004; received in revised form 23 July 2004; accepted 12 August 2004
Available online 7 October 2004

Abstract

We develop solutions for the transport of suspended sediment by a single swash event following the collapse of a bore on a plane beach, and we investigate the morphodynamical role that such transport may play. Although the intrinsic asymmetry between uprush and backwash velocities tends to encourage the export of sediment, we find that swash events may be effective in distributing across the swash zone much or all of the sediment mobilised by bore collapse; additionally, settling lag effects may promote a weak onshore movement of sediment. We quantify both effects in terms of the properties of the sediment and of the swash event, and comment on the relationship between our findings and recent field studies of swash zone sediment transport.

Keywords: Swash zone; Suspended sediment transport; Beach morphodynamics; Wave run-up

1. Introduction and motivation

When waves break and collapse on a beach they drive rapid, shallow flows under which the shoreline moves back and forwards across the so-called 'swash zone' of the beach. These swash events may be a significant agent of sediment transport on many natural beaches, but because of the difficulties in measuring hydrodynamic quantities and sediment transport in very shallow water, as well as the highly transient nature of the flows and the strongly non-linear nature of sediment transport processes, their role is not fully understood.

In recent years, considerable efforts have been made to improve the state of knowledge of swash zone transport processes (see the reviews by Butt and Russell, 2000 and Elfrink and Baldock, 2002). Several important aspects, however, remain outstanding. In particular, there is uncertainty about the structure of

* Corresponding author.
E-mail addresses: david@bpi.cam.ac.uk (D. Pritchard), a.j.hogg@bris.ac.uk (A.J. Hogg).

0378-3839/$ - see front matter © 2004 Elsevier B.V. All rights reserved.
doi:10.1016/j.coastaleng.2004.08.002

the turbulence in the flow which follows wave breaking (Longo et al., 2002; Petti and Longo, 2001); about the role of beachface permeability (Elfrink and Baldock, 2002; Butt et al., 2001); and about how the modes of sediment transport should be described. Although this latter point is often treated as a matter of nomenclature, the distinction between bedload and suspended load is of considerable importance for morphodynamic purposes. Even in steady flow, the transport rates of material carried as bed and as suspended load may be rather different and depend differently on the hydrodynamic variables. In unsteady flows, a more fundamental difference is that suspended load does not respond instantaneously to changes in the flow conditions, and this may lead to net cross-shore transport through settling lag effects (see, e.g., Pritchard and Hogg, 2003a), which do not occur for bedload. A further reason to consider suspended load is that a considerable amount of sediment may be suspended by the intense turbulence which occurs during wave collapse (Elfrink and Baldock, 2002; Kobayashi and Lawrence, 2004), and at least some will settle out during the uprush, leading to a net landward movement of sediment. Thus, although suspended sediment load may be smaller than bedload during most phases of a swash event (we note that even this is hard to confirm in the field), its different behaviour may give it a rather different, and perhaps more significant, morphodynamic role. The numerical study of Kobayashi and Johnson (2001) has suggested that including suspended load improves the ability of a sediment transport model to predict morphological changes, while the recent numerical and field investigation of Jackson et al. (2004) has for the first time attempted to identify the different contributions to cross-shore transport from locally mobilised sediment and from that 'pre-suspended' by the bore collapse.

Motivated by these experimental and numerical findings, in the current study, we carry out an analytical investigation of suspended sediment transport under a single swash event. We consider separately the roles of lag effects and of sediment supply from the bore collapse, and, following Jackson et al. (2004), we pay particular attention to the spatial distribution of sediment transport. Our results provide an easily reproduced prediction of suspended sediment transport in the swash zone, which may act as a baseline result for future experimental and numerical studies. In particular, they indicate that the amount of sediment which is initially suspended by the bore is crucially important in determining the direction of net transport, and they provide estimates of how much sediment must be pre-suspended in order for its onshore advection and deposition to counterbalance the tendency of the swash zone to export sediment.

We employ the model of a swash event obtained by Shen and Meyer (1963) as a solution to the depth-averaged shallow-water hydrodynamic equations, and we use a similarly reduced model for suspended sediment transport. Shen and Meyer's solution provides a good description of swash flow (see, e.g., Barnes, 1996; Titov and Synolakis, 1995), although some numerical studies (e.g., Hibberd and Peregrine, 1979) have suggested that additional frictional and non-hydrostatic effects should be included to obtain better agreement with experimental data. It has also proved useful in the interpretation of more complex swash motions (see, e.g., Baldock and Holmes, 1999), suggesting that it captures many of the essential aspects of swash flow. Finally, it is an important benchmark problem for numerical methods which complements the more elaborate non-breaking solutions based on the formalism of Carrier and Greenspan (1958).

In Section 2, we describe a depth-averaged model of sediment transport and present the hydrodynamic solution of Shen and Meyer (1963). A key feature of this sediment transport model is that it does not depend on any heuristic parameters, so all input quantities can in principle be measured independently. In Section 3, we consider the transport predicted under Shen–Meyer flow by a quasi-steady 'total load' model. In Section 4, we consider transport when the quasi-steady assumption is abandoned: in particular, we consider the onshore transport of sediment suspended by the initial bore collapse, and the role of lag effects. We discuss these results in some detail in Section 5, and relate them to recent field studies as well as to other modelling approaches. Finally, in Section 6, we summarise our conclusions from this study. Appendix A gives details of some mathematical results which help to interpret and generalise our findings.

2. Development of the model

2.1. The shallow-water equations

Working in a shallow-water framework (Peregrine, 1972), we describe the flow in terms of its depth $\hat{h}$ normal to the bed and depth-averaged velocity $\bar{u}$ parallel to the bed. Suspended sediment is described in terms of a depth-averaged mass concentration $\bar{c}$. The bed is taken to be planar with an inclination θ to the horizontal: $\hat{x}$ is a bed-parallel distance which increases inland. (Carets and overbars both denote dimensional quantities, while dimensionless quantities are unadorned.)

The flow and transport are governed by the dimensional equations

$$\frac{\partial \hat{h}}{\partial \hat{t}} + \frac{\partial (\bar{u}\hat{h})}{\partial \hat{x}} = 0 \tag{1}$$

$$\frac{\partial \bar{u}}{\partial \hat{t}} + \bar{u}\frac{\partial \bar{u}}{\partial \hat{x}} + \hat{g}\cos\theta \frac{\partial \hat{h}}{\partial \hat{x}} = -\hat{g}\sin\theta \tag{2}$$

and

$$\frac{\partial \bar{c}}{\partial \hat{t}} + \bar{u}\frac{\partial \bar{c}}{\partial \hat{x}} = \frac{\hat{m}_e q_e - \hat{w}_s \bar{c}}{\hat{h}}. \tag{3}$$

Eqs. (1) and (2) represent the conservation of fluid mass and fluid momentum respectively, while Eq. (3) is a depth-integrated transport equation for suspended sediment (see, e.g., Pritchard and Hogg, 2003b). We have used the result that the horizontal velocity is vertically uniform to leading order (Peregrine, 1972; Petti and Longo, 2001) to write the fluxes of momentum and suspended sediment in terms of the depth-averaged quantities $\bar{u}$ and $\bar{c}$. We neglect the horizontal diffusion of suspended sediment, which in a shallow-water regime is expected to be small compared to the advective transport, and we assume that the beach morphology does not change appreciably over the timescale of a swash event.

We have also neglected any effect from the percolation of water into and out of the beachface. For beaches of coarse sand or gravel, this process is likely to influence the hydrodynamics significantly, and may also affect sediment transport directly by stabilising or destabilising the bed and by altering the mass transport rate in the near-bed region (Conley and Inman, 1994; Butt et al., 2001). However, a detailed numerical study (Masselink and Li, 2001) has indicated that for beaches of grain size less than about 1 mm, swash infiltration is not an important effect, because the hydraulic conductivity of the beachface decreases with sediment size. The results obtained here, therefore, are most appropriate for beaches of medium sand or finer.

The right-hand side of Eq. (3) represents the erosion and deposition of sediment. The first term, $\hat{m}_e q_e$, is a mass erosion rate per unit area of the bed. In the second (depositional) term, $\hat{w}_s$ is the effective settling velocity of the sedimentary particles. If we assume a vertically well-mixed suspension, $\hat{w}_s$ is identical to the settling velocity of an individual particle; however, it may also be used to represent settling from a vertically structured suspension, in which case it is increased by the ratio of the near-bed concentration to the vertically averaged concentration (Pritchard and Hogg, 2003b). The form of this weighting depends on the assumptions made about the vertical distribution of sediment in the water column, and thus on the detailed turbulence structure of the flow; recent work by Masselink et al. (2004) has suggested that concentration may be represented by an exponential distribution with a mixing length of 2–3 cm, so for flows a few centimetres deep, the effective settling velocity could increase by a factor of up to 10. [However, if very high concentrations are attained in the near-bed region, this can reduce the effective settling velocity because of hindered settling effects (see Baldock et al., 2004).] We will discuss below how the uncertainty in this component of the model affects our results.

In principle, we could consider almost any form of the mass erosion rate q_e as a function of the hydrodynamic conditions. In the current study, we restrict ourselves to considering erosion rates of the form

$$\hat{m}_e q_e = \hat{m}_e \left(\frac{|\hat{\tau}| - \hat{\tau}_e}{\hat{\tau}_0} \right)^n, \tag{4}$$

where $n>0$, where $\hat{\tau}_e$ and $\hat{\tau}_0$ are a threshold stress for erosion and a reference shear stress, respectively, and where the relation is presumed to hold only when $|\hat{\tau}|>\hat{\tau}_e$; for $|\hat{\tau}|<\hat{\tau}_e$, no erosion occurs. The effective bed shear stress is calculated using the Chezy law $\hat{\tau}=c_D\hat{\rho}|\bar{u}|\bar{u}$ where c_D is a small, constant friction coefficient; more complex closures could

readily be employed, and in Section 3.1, we will consider what happens when the assumption of a constant c_D is relaxed slightly.

We define the instantaneous and net sediment fluxes by

$$\bar{q}(\hat{x},\hat{t}) \equiv \hat{h}(\hat{x},\hat{t})\bar{u}(\hat{x},\hat{t})\bar{c}(\hat{x},\hat{t}) \quad \text{and}$$

$$\hat{Q}(\hat{x}) \equiv \int_{\hat{t}_{in}(\hat{x})}^{\hat{t}_{de}(\hat{x})} \bar{q}(\hat{x},\hat{t})\mathrm{d}\hat{t}, \tag{5}$$

where the limits of integration represent the times of inundation and denudation of the point $\hat{x}$. $\hat{Q}(\hat{x})$ then describes the net transport of sediment across the swash zone under a single swash event; specifically, $\hat{Q}(0)$ is the net mass of sediment per unit cross-stream width which is imported to the swash zone by this event. The net deposition at a point over one swash event is proportional to the first derivative of the net flux: If the mass concentration of sediment in the bed is given by $\hat{c}_b$, the depth of net deposition will be given by

$$\hat{\eta}(\hat{x}) = -\frac{1}{\hat{c}_b}\frac{\mathrm{d}\hat{Q}}{\mathrm{d}\hat{x}}. \tag{6}$$

The suspended load model described here differs from conventional bedload and total load models (e.g., Bagnold, 1966; Bailard, 1981) in that the rate of sediment transport is not an instantaneous function of the hydrodynamic variables $\bar{u}$ and $\hat{h}$; instead, changes in the suspended sediment load will tend to lag behind changes in the forcing conditions with a characteristic 'response time' $\hat{t}_r$ of the order of $\hat{h}/\hat{w}_s$ (Stansby and Awang, 1998). Under steady flow conditions, or when $\hat{t}_r$ is very small compared to the timescale over which the flow changes, $\bar{c}$ will tend to adopt an equilibrium value $\hat{c}_{eq}(\hat{\tau})=\hat{m}_e q_e(\hat{\tau})/\hat{w}_s$ at which erosion precisely balances deposition. The mass flux of suspended sediment will then be given by the quasi-steady expression $\bar{u}\hat{h}\hat{c}_{eq}$. This resembles a conventional total load formula except for the dependence of the transport rate on $\hat{h}$. We will show in Sections 3 and A.1 that this dependence does not greatly alter the character of the transport processes; the existence of a finite response time, however, makes a more fundamental difference.

2.1.1. Non-dimensionalisation

Following Peregrine and Williams (2001), we scale hydrodynamic quantities on the vertical excursion 2Â of the swash, and following Pritchard and Hogg (2003b), we choose the natural concentration scale $\hat{C}=\hat{m}_e/\hat{w}_s$. The dimensionless variables are then

$$x = \frac{\hat{x}\sin\theta}{\hat{A}}, \quad t = \hat{t}\sin\theta\sqrt{\frac{\hat{g}}{\hat{A}}}, \quad h = \frac{\hat{h}\cos\theta}{\hat{A}},$$

$$u = \frac{\bar{u}}{\sqrt{\hat{g}\hat{A}}} \quad \text{and} \quad c = \frac{\bar{c}}{\hat{C}}, \tag{7}$$

while the governing equations become

$$\frac{\partial h}{\partial t} + \frac{\partial (uh)}{\partial x} = 0, \quad \frac{\partial u}{\partial t} + u\frac{\partial u}{\partial x} + \frac{\partial h}{\partial x} = -1 \tag{8}$$

$$\text{and} \quad \frac{\partial c}{\partial t} + u\frac{\partial c}{\partial x} = E\frac{q_e - c}{h},$$

$$\text{where} \quad E \equiv \frac{\hat{w}_s}{\tan\theta\sqrt{\hat{g}\hat{A}}}. \tag{9}$$

The 'exchange rate' parameter E gives a global estimate of the ratio of the hydrodynamic timescale to the sediment response timescale $\hat{t}_r$, and so quantifies how sediment transport lags behind changes to the hydrodynamic variables. The local sediment lag, however, may vary considerably in time and space, since it depends both on the local fluid acceleration and on the local fluid depth which determines $\hat{t}_r$.

To determine what range of E we should consider, we take as a reference case a steep beach with $\tan\theta=0.1$. Maximum velocities under swash may range from about 0.5 m s^{-1} to as much as 4 m s^{-1} for a particularly vigorous event, which as we will see corresponds to the velocity scale $\sqrt{\hat{g}\hat{A}} = 0.25$ to 2 m s^{-1}. As indicated above, we are concerned primarily with beaches of fine to medium sand, for which we may take $\hat{w}_s \approx 10^{-2}$ m s^{-1}; it is also interesting to consider the fate of finer particles, to determine whether these can be preferentially removed from beaches as suspended load, and so we may reasonably consider $\hat{w}_s$ as low as 10^{-3} m

s^{-1}. These reference values suggest that we should consider a range of E from around 0.005 to 0.4: we will first show some examples from the extremes of this range, and investigate the dependence of our results on E more thoroughly later, when we will also discuss the effect of allowing for the vertical structure of the concentration field. (Most of our discussion will refer to the nondimensional form of the results, but in Section 4.4.1, we will return to this reference case to estimate dimensional values for the expected rates of erosion and accretion under swash.)

Using Eq. (7), the nondimensional erosion rate is given by

$$q_e = \begin{cases} (u^2 - u_e^2)^n & \text{when} \quad |u| \geq u_e, \\ 0 & \text{when} \quad |u| < u_e, \end{cases}$$

$$\text{where } u_e \equiv \sqrt{\frac{\hat{\tau}_e}{c_D \hat{\rho} \hat{g} \hat{A}}}. \tag{10}$$

Finally, the dimensionless fluxes have the form

$$q(x,t) \equiv h(x,t)u(x,t)c(x,t) \quad \text{and}$$

$$Q(x) \equiv \int_{t_{in}(x)}^{t_{de}(x)} q(x,t)\mathrm{d}t. \tag{11}$$

2.1.2. Lagrangian formulation

The Lagrangian method introduced by Pritchard and Hogg (2002) allows the governing equations for suspended sediment transport to be integrated either numerically or analytically for any known flow field. In this approach, we write Eq. (9a) in Lagrangian form, following a fluid element with position $x_L(t; \xi)$ which carries sediment concentration $c_L(t; \xi) = c(x_L(t; \xi), t)$, where ξ is a parameter which labels the elements. We obtain two first-order ordinary differential equations,

$$\frac{\mathrm{d}x_L}{\mathrm{d}t} = u(x_L, t) \quad \text{with} \quad x_L(t_0(\xi)) = x_0(\xi), \tag{12}$$

$$\text{and} \quad \frac{\mathrm{d}c_L}{\mathrm{d}t} = E\frac{q_e(u(x_L,t)) - c_L(t)}{h(x_L,t)} \quad \text{with}$$

$$c_L(t_0(\xi)) = c_0(\xi). \tag{13}$$

2.2. Shen and Meyer's solution for a swash event

As part of a series of mathematical studies of wave breaking on a plane beach, Shen and Meyer (1963) obtained an exact solution to the shallow-water equations which describes the flow following bore collapse on a plane beach. This solution may be interpreted in several ways. It is most correct to regard it as an asymptotic description, valid for a very wide class of initial conditions, of the flow field close to the moving shoreline. In this context, the most important aspect of the solution is that the shoreline undergoes so-called 'ballistic' motion with a constant downslope acceleration due to gravity: this result has been widely used in the interpretation of swash zone processes (see, e.g., Baldock and Holmes, 1999).

Alternatively, Shen and Meyer's flow field may be interpreted as an exact solution for either an initial value problem or a boundary value problem. In the initial condition interpretation, the fluid is initially at rest, with uniform depth $h=1$ behind a 'dam' at $x=0$; at $t=0$, the dam is removed and the fluid is allowed to flow out and to accelerate downslope. In the boundary condition interpretation, we consider only the flow in some region close to the shoreline, and regard the flow as 'driven' by incoming characteristics which satisfy the condition $u + 2\sqrt{h} + t = 2$. Although we will generally describe results in terms of the boundary value problem, the initial value interpretation is useful because it provides a natural way to label Lagrangian fluid elements (see below).

The derivation of the solution has been succinctly described by Peregrine and Williams (2001). In dimensionless variables, it has the form

$$h(x,t) = \frac{(4t - t^2 - 2x)^2}{36t^2} \quad \text{and}$$

$$u(x,t) = \frac{2}{3t}\left(t - t^2 + x\right) \tag{14}$$

in the region $-t - \frac{1}{2}t^2 < x < 2t - \frac{1}{2}t^2$. Meanwhile, the notional 'reservoir' region behind $x = -t - \frac{1}{2}t^2$ accelerates downslope with uniform depth $h=1$ and increasing negative velocity $u=-t$. The times of

inundation and denudation of a point x are given respectively by

$$t_{\mathrm{in}}(x) = 2 - \sqrt{4 - 2x} \quad \text{and} \quad t_{\mathrm{de}}(x) = 2 + \sqrt{4 - 2x}. \tag{15}$$

It is useful also to note here the convective acceleration field $\mathrm{D}u/\mathrm{D}t$, which is given by

$$\frac{\mathrm{D}u}{\mathrm{D}t}(x,t) = \frac{\partial u}{\partial t} + u\frac{\partial u}{\partial x} = \frac{2}{9}\frac{2t - 5t^2 - x}{t^2}. \tag{16}$$

2.2.1. Region of validity of the solution

Shen and Meyer's swash solution, like the classical dam-break solution (Ritter, 1892), becomes singular at $(x, t)=(0, 0)$, where the free surface becomes vertical (the 'dam') and the acceleration of the shoremost fluid element becomes unbounded, since it must accelerate from rest to a velocity of 2 instantaneously. This singularity means that there is a region around (0, 0) in which the shallow-water approximations are no longer valid. This region may most easily be defined as that in which $|\partial h/\partial x| = |\mathrm{D}u/\mathrm{D}t + 1|$ is greater than some small quantity ϵ_2, yielding the criterion

$$x < x_{\mathrm{val}}(t;\varepsilon) = 2t - \frac{1}{2}t^2 - \epsilon t^2 \tag{17}$$

for invalidity, where $\epsilon = 9\epsilon_2/2$. (We note that setting $\epsilon = 9(\epsilon_1/10)^{1/2}$ recovers the essentially equivalent definition used by Peregrine and Williams (2001), where ϵ_1 is the acceleration of a water particle perpendicular to the beach.)

Although the shallow-water approximations are strictly valid only when $\epsilon_2 \ll 1$, we expect the Shen–Meyer solution, like the related horizontal dam-break solution to the shallow-water equations, to apply reasonably well even when this is not strictly satisfied. The experiments of Stansby et al. (1998) suggest that the exact solution for horizontal dam-break flow provides a reasonable description of the flow once $|\partial h/\partial x| \lesssim 1$, despite the effects of strongly non-hydrostatic pressures at earlier stages. (Jensen et al. (2003) have considered the use of a Boussinesq approximation as a first step towards describing these.) Seaward of $x \approx x_{\mathrm{val}}(t;\ \epsilon_2 = 1)$, the flow may be strongly three-dimensional and unsteady, owing its structure to the interaction between the collapsing bore and the backwash of the previous swash event (see, e.g., Cowen et al., 2003; Matsunaga and Honji, 1980), and the shallow-water model cannot be expected to capture the processes in this region. It may therefore be natural to treat x_{val} as a natural boundary on which to impose a boundary condition on suspended sediment, representing the amount stirred up by the complex three-dimensional flow which follows the collapse of the bore. We will return to this point in the next section.

2.2.2. Lagrangian form of the solution

It is straight forward to construct the trajectory of a fluid element. We label fluid elements $x_{\mathrm{L}}(t;\ \xi)$ such that in the 'dam-break' interpretation of the solution, $x_{\mathrm{L}}(0;\ \xi) = \xi < 0$. Using $\mathrm{d}x_{\mathrm{L}}/\mathrm{d}t = u(x_{\mathrm{L}},\ t)$, we obtain

$$x_{\mathrm{L}}(t;\xi) = \begin{cases} \xi - \frac{1}{2}t^2 & \text{for} \quad t < |\xi| \\ 2t - \frac{1}{2}t^2 - 3|\xi|^{1/3}t^{2/3} & \text{for} \quad t \geq |\xi|, \end{cases} \tag{18}$$

and thus the velocity

$$u_{\mathrm{L}}(t;\xi) \equiv u(x_{\mathrm{L}}(t),t) = \begin{cases} -t & \text{for} \quad t < |\xi| \\ 2 - t - 2|\xi|^{1/3}t^{-1/3} & \text{for} \quad t \geq |\xi|; \end{cases} \tag{19}$$

the depth

$$h_{\mathrm{L}}(t;\xi) \equiv h(x_{\mathrm{L}}(t),t) = \begin{cases} 1 & \text{for} \quad t < |\xi| \\ |\xi|^{2/3}t^{-2/3} & \text{for} \quad t \geq |\xi|; \end{cases} \tag{20}$$

and the convective acceleration

$$\frac{\mathrm{D}u}{\mathrm{D}t} = \frac{\mathrm{d}u_{\mathrm{L}}}{\mathrm{d}t} = \begin{cases} -1 & \text{for} \quad t < |\xi| \\ -1 + \frac{2}{3}|\xi|^{1/3}t^{-4/3} & \text{for} \quad t \geq |\xi|. \end{cases} \tag{21}$$

Shen and Meyer's solution is illustrated in Fig. 1a, while Fig. 1b shows the fluid trajectories $x_{\mathrm{L}}(t)$. The swash event is dominated by very shallow flows; we also note that while the shoreline reverses direction at $t=2$ and follows a symmetrical 'ballistic' trajectory, fluid elements behind it reverse direction sooner.

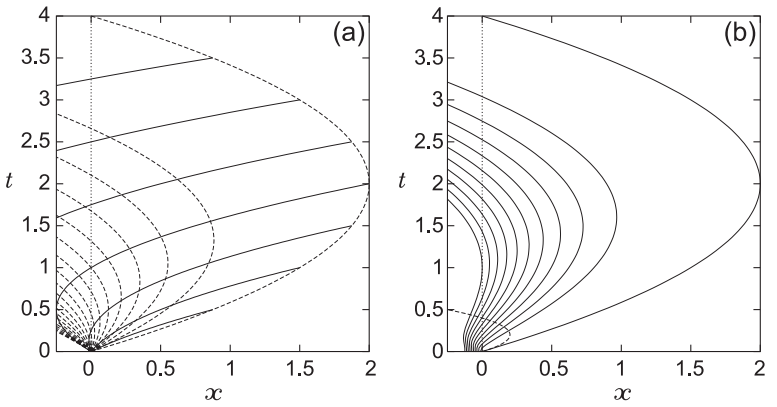

Fig. 1. Important features of Shen and Meyer's swash solution. (a) Eulerian form of the (nondimensional) solution: contours of constant u (solid lines: $u=-1.5$ to 1.5 by 0.5) and constant h (dashed lines: $h=0$ to 1 by 0.05). (b) Lagrangian fluid element trajectories $x_L(t)$ (solid lines) and border $x_{val}(t)$ (dashed line) of region in which $|\partial h/\partial x|>1$. Note the narrow range $x_L(0)=-1/8$ to 0 of elements which enter the region $x>0$ at some point.

Consequently, the speed of a fluid element is reduced relative to ballistic motion $u=2-t$ on the uprush, and increased on the backwash. Thus there is an intrinsic asymmetry in the hydrodynamics that we may expect to favour the export of sediment from the swash zone. However, this tendency may be counterbalanced by landwards transport through settling lag effects (cf. Pritchard and Hogg, 2003a) or by the presence of high levels of pre-suspended sediment which are advected into the swash zone: this latter mechanism was identified as important by both Nielsen (2002) and Kobayashi and Lawrence (2004). In the following sections, we will consider firstly transport under a steady-state total load model (Section 3) which illustrates the effect of the hydrodynamic asymmetry, and secondly transport under the non-equilibrium suspended load model (Section 4) which includes both pre-suspended sediment and settling lag.

3. Steady-state transport

Many studies of sediment transport in the swash zone have employed a 'total load' description of sediment transport, in which the total sediment flux is taken to be a function of the instantaneous or time-averaged hydrodynamic variables (e.g., Bailard, 1981). This lacks two features which our suspended load formulation contains: firstly, the supply of sediment mobilised by the initial bore and advected into the swash zone; and secondly, the potential for net transport which arises from lag effects. A principal aim of this study is to investigate the contribution of these two mechanisms to net sediment fluxes, and so it is useful to consider as a baseline the case in which neither applies. This arises naturally when the quantity E/h in the sediment transport Eq. (9) is much greater than 1 (i.e., in very shallow water or for very coarse sediment), so that $c(x,t)=c_{eq}(u(x,t))$ everywhere, and $q=q_{eq}=c_{eq}uh$. $Q(x)$ may then be calculated by the simple integration

$$Q_{eq}(x)=\int_{t_{in}(x)}^{t_{de}(x)} h(x,t)u(x,t)c_{eq}(x,t)\mathrm{d}t. \qquad (22)$$

Representative results for several forms of the sediment transport rate are shown in Figs. 2 and 3. The overall transport pattern is remarkably invariant as q_{eq} is varied; in each case, the onshore flux during the uprush peaks within the lower part of the swash zone before dying away rapidly upslope, while the offshore flux on the backwash increases strongly seawards. The net result in each case is that sediment is exported from the swash zone, and as Fig. 3 illustrates, the principal reason is that the backwash lasts longer than the uprush, and the higher concentrations on the uprush fail to compensate for this effect. This result is very robust to the form of the total load transport model employed: we show in Section A.1 that it will hold for any model in which the flux is

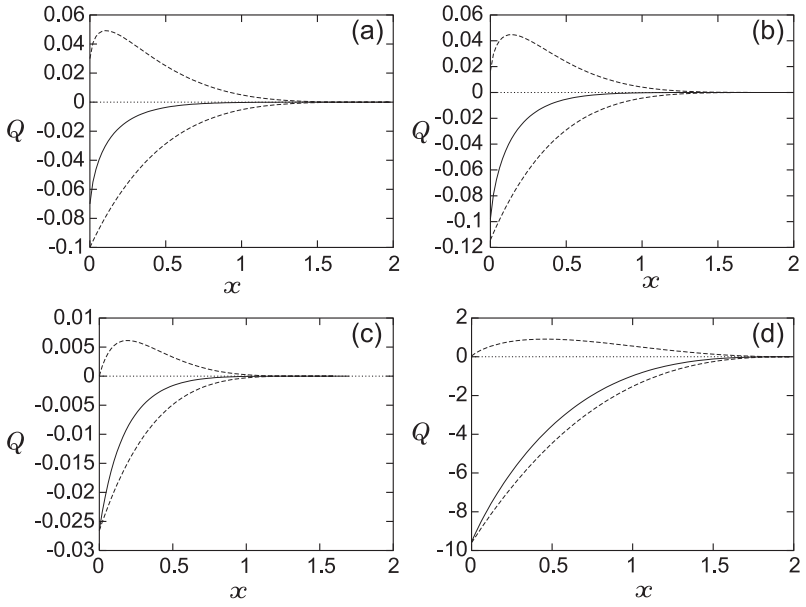

Fig. 2. Non-dimensional net fluxes $Q_{eq}(x)$ for (a) $q_{eq}=u^2uh$; (b) $q_{eq}=|u^3|uh$; (c) $q_{eq}=(u^2-1)uh$ when $|u|>1$; (d) $q_{eq}=|u^3|u$ (Bailard model). Solid lines represent net flux over a cycle; dashed lines represent net contributions from uprush and backwash separately.

an increasing function of $|u|$, whether or not the flux also depends on h. This confirms the intuitive result that if lag effects and pre-suspension are neglected, the asymmetry between uprush and backwash in this flow should tend to lead to the export of sediment by a swash event. It is also consistent with the numerical results of Masselink and Li (2001) for a beach of negligible permeability: they found that starting from a plane beach, sediment was eroded consistently from the swash zone and was deposited seaward of the swash zone at around 1 m depth below the undisturbed water level (see Fig. 8a of Masselink and Li, 2001).

In our suspended load formulation, the sediment flux q depends on the depth h of the water, whereas in Bailard's (1981) total load formulation, q is independent of h. (Bagnold, 1966 notes that this is a deficiency in the standard energetics-based transport model, since it suggests that a vanishingly small amount of water can transport a non-vanishing quantity of sediment.) As Fig. 2d illustrates, this independence does not make a great difference to the overall transport pattern, although it does extend the influence of the swash further upslope where depths are very low. Fig. 3b illustrates that when q is independent of h the transport rate is highest at the

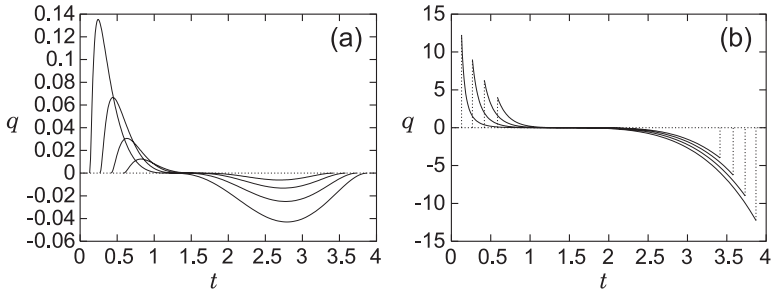

Fig. 3. Non-dimensional instantaneous fluxes $q_{eq}(x, t)$ plotted at x=0.25, 0.5, 0.75 and 1, for (a) $q_e=|u^2|uh$; (b) $q_e=|u^3|u$ (Bailard model).

moments of inundation and denudation; however, the mechanism leading to net transport remains essentially the same.

We also note that the presence of even a relatively high critical shear stress for erosion (Fig. 2c) makes no qualitative difference to the pattern of net transport. In future sections, we will take as a reference case the simplest form of the erosion rate, u_e=0 and n=2, though we will also consider alternative values of u_e and n.

3.1. The effect of a varying friction coefficient

So far, our discussion has assumed that the friction coefficient c_D in the Chezy drag law is a constant, and in particular that it has the same value during the uprush and during the backwash. This is a simplification of the physics of swash zone turbulence, and while it lies beyond the current study to examine in detail how employing a varying friction factor in a swash model might affect sediment transport patterns, it is worth paying some attention to this question.

Several previous studies have suggested that the shear stresses exerted on the bed by a given free stream velocity might differ on the uprush and the backwash, and that this might explain a bias towards onshore sediment transport (Masselink and Hughes, 1998). Such a difference in friction coefficients can be seen as a simple model of the developing boundary layer under the flow. It is only very recently, however, that direct measurements of this effect have become available. The field study by Conley and Griffin (2004) suggests that c_D is a weak function of Reynolds number and that, more significantly, the values on the backwash may be systematically as much as 50% lower than those on the uprush. For simplicity, we will consider only the latter effect here.

It is simple to include a directionally dependent friction coefficient in the model described here for steady-state transport. Defining β<1 to be the ratio of the backwash to the uprush friction coefficient and $t_0(x)$ to be the time such that $u(x, t_0)$=0, we obtain

$$Q_{\mathrm{eq}}(x) = \int_{t_{\mathrm{in}}(x)}^{t_0(x)} h(x,t)u(x,t)\left(u^2 - u_{\mathrm{e}}^2\right)^n \mathrm{d}t + \int_{t_0(x)}^{t_{\mathrm{de}}(x)} h(x,t)u(x,t)\left(\beta u^2 - u_{\mathrm{e}}^2\right)^n \mathrm{d}t \quad (23)$$

for an equilibrium suspended-load model, and

$$Q_{\mathrm{eq}}(x) = \int_{t_{\mathrm{in}}(x)}^{t_0(x)} u(x,t)^4 \mathrm{d}t - \beta \int_{t_0(x)}^{t_{\mathrm{de}}(x)} u(x,t)^4 \mathrm{d}t \quad (24)$$

for a Bailard-type model.

Fig. 4 shows some typical results for each case. The effect of introducing an asymmetry in c_D is felt most close to maximum run-up, where there is a more delicate balance between the magnitudes of transport on the uprush and the backwash (cf. Section A.2), and it can be shown (Section A.2.1) that for any β<1, there must be a region of weak onshore transport in the upper part of the swash zone. Meanwhile, a much lower value of β is required to reverse transport at the seaward end of the swash zone: for u_e=0 and m=2 or 3, net transport must remain seawards here for $\beta \gtrsim 0.3$, while under the Bailard model, any value of β>1/243 will lead to net offshore transport here. Fig. 4b indicates how much stronger the bias in favour of offshore transport is in the Bailard model: with β=0.5,

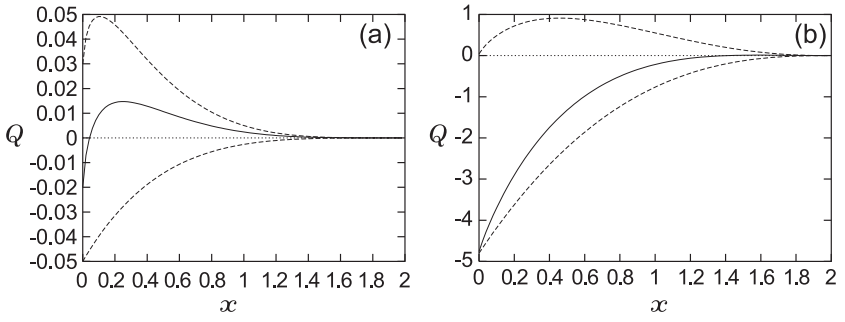

Fig. 4. Non-dimensional net fluxes $Q_{\mathrm{eq}}(x)$ for (a) u_e=0, n=1 and β=0.5; (b) Bailard model with β=0.5. Solid lines represent net flux over a cycle; dashed lines represent net contributions from uprush and backwash separately.

the region of net onshore transport is confined to the uppermost part of the swash zone and is extremely weak, whereas the same value of β causes appreciable onshore transport and sediment divergence under an equilibrium suspended-load model (Fig. 4a).

The overall conclusion of this brief discussion is that for the range of values of β suggested by Conley and Griffin's measurements, we expect friction factor asymmetry to lead to sediment divergence in the swash zone, but not to explain net landwards transport throughout it.

4. Non-steady-state transport

We now extend the analysis to consider situations in which the suspended sediment load takes a finite 'lag' time to respond to changes in the hydrodynamic conditions, and in which there may be sediment already in suspension at the start of the swash event.

4.1. Lagrangian method of solution

We may write the Lagrangian equation for concentration following a fluid element as

$$\frac{\mathrm{d}c_\mathrm{L}}{\mathrm{d}t} + \frac{E}{h_\mathrm{L}(t)} c_\mathrm{L}(t) = \frac{E q_\mathrm{e}(u_\mathrm{L}(t))}{h_\mathrm{L}(t)}. \tag{25}$$

The solution satisfying $c_\mathrm{L}(t_0(\xi))=c_0(\xi)$ has the form $c_\mathrm{L}(t;\,\xi)=c_0(\xi)c_\mathrm{L}^{\mathrm{pr}}(t;\,\xi)+c_\mathrm{L}^{\mathrm{en}}(t;\,\xi)$, where

$$c_\mathrm{L}^{\mathrm{pr}}(t;\xi) = \Omega(t, t_0(\xi)) \quad \text{where}$$

$$\Omega(t, t_0) = \exp\left[- \int_{t_0}^{t} \frac{E}{h_\mathrm{L}(t')} \mathrm{d}t' \right], \text{and}$$

$$c^{\mathrm{en}}(t;\xi) = \Omega(t, t_0(\xi)) \int_{t_0(\xi)}^{t} \frac{1}{\Omega(t', t_0(\xi))} \frac{E q_\mathrm{e}(t')}{h_\mathrm{L}(t')} \mathrm{d}t' \,. \tag{26}$$

With an appropriate choice of c_0 and t_0 as functions of the element labelling quantity ξ, we can then use Eq. (26) to represent the concentration field subject to an initial or boundary condition of the form $c_\mathrm{L}(t_0(\xi);\,\xi)=c_0(\xi)$ on some curve $\mathcal{C}_{bdy} = (x_0(\xi), t_0(\xi))$ such that $\mathcal{C}_{bdy}$ is never tangent to any of the trajectories $(x_\mathrm{L}(t;\,\xi),\,t)$. As special cases, we may choose either of the curves $x_0=0$ or $x_0(t_0)=x_{\mathrm{val}}(t_0;\,\epsilon_2=1)=2t_0-5t_0^2$, and impose $c(x_0,\,t)$ during the inflow phase when $u(x_0,\,t_0)>0$. (We will show that the difference between imposing a boundary condition at $x=0$ and at $x=x_{\mathrm{val}}$ is minimal.) Finally, the Eulerian solution is obtained by using Eq. (18) and the definition of $t_0(\xi)$ to substitute $\xi(x,\,t)$ into each part of the Lagrangian solution $c_\mathrm{L}(t;\,\xi)$.

Splitting the solution into the components c^{pr} and c^{en} has an immediate physical interpretation. The quantity $c_\mathrm{L}^{\mathrm{en}}\,(t;\,\xi)$ represents sediment that is entrained within the swash zone, while $c_\mathrm{L}^{\mathrm{pr}}(t;\,\xi)$ represents sediment that is pre-suspended by the bore and input to the swash event along the boundary $\mathcal{C}_{bdy}$, and which gradually deposits. It is useful to separate these two contributions to net transport in this way, because it provides an immediate means of determining when swash zone transport is dominated by sediment mobilised by the initial bore and when it is dominated by the swash flow itself (Jackson et al., 2004). We will denote all quantities which refer to the pre-suspended sediment by a superscript $^{\mathrm{pr}}$ and those which refer to sediment entrained within the swash zone by a superscript $^{\mathrm{en}}$.

Eq. (26) may be evaluated exactly for some specific choices of q_e. In general, however, it is most efficient to evaluate it numerically using a computer algebra package such as MAPLE or a standard numerical integration routine (Press et al., 1992). Both methods were employed to generate the results presented here.

It is also helpful to obtain approximations to Eq. (26) in the limits of large and small E. As we have already noted, in the limit of large E, the suspended sediment concentration stays very close to its equilibrium value c_{eq}. We can then describe the suspended sediment concentration by an asymptotic expansion valid for large E,

$$c(x,t) = c_{\mathrm{eq}}(u(x,t)) + \frac{1}{E} c_1(x,t) + \mathcal{O}\left(E^{-2}\right), \tag{27}$$

where it can be shown by direct substitution into the governing transport equation that

$$\begin{aligned} c_1(x,t) &= -h(x,t)\left(\frac{\partial c_{\mathrm{eq}}}{\partial t} + u \frac{\partial c_{\mathrm{eq}}}{\partial x} \right) \\ &= -h \frac{\mathrm{d}c_{\mathrm{eq}}}{\mathrm{d}u} \frac{\mathrm{D}u}{\mathrm{D}t}. \end{aligned} \tag{28}$$

We note that this expansion reduces the order of the problem and does not allow an initial condition on c to be imposed. However, it is valid in particular in the very small depths around the point of maximum run-up: we make use of this fact in Section A.2 to obtain results for the net sediment transport in the upper part of the swash zone.

It is also useful to develop approximate solutions in the regime of small E (very slow sediment response): in this regime we may expand Eq. (26) to give

$$c_{\mathrm{L}}^{\mathrm{pr}}(t;\xi) = c_0(\xi) + E\int_{t_0(\xi)}^{t} \frac{q_{\mathrm{e}}(u_{\mathrm{L}}(t';\xi)) - c_0(\xi)}{h_{\mathrm{L}}(t';\xi)}\,\mathrm{d}t' + \mathcal{O}\left(E^2\right) \tag{29}$$

$$\text{and} \quad c_{\mathrm{L}}^{\mathrm{en}}(t;\xi) = E\int_{t_0(\xi)}^{t} \frac{q_{\mathrm{e}}(u_{\mathrm{L}}(t';\xi))}{h_{\mathrm{L}}(t';\xi)}\,\mathrm{d}t' + \mathcal{O}\left(E^2\right). \tag{30}$$

Consequently, in this regime, all net fluxes are proportional to E to leading order.

4.2. Examples of solutions for sediment entrained within the swash zone

We start by considering the solutions for sediment which is entrained within the swash zone. Figs. 5 and 6 show how the concentration field $c^{\mathrm{en}}(x, t)$ evolves for two different values of E, while Figs. 7 and 8 illustrate the corresponding Eulerian sediment fluxes $q^{\mathrm{en}}(x, t)$ and $Q^{\mathrm{en}}(x)$. (Hereafter, unless otherwise stated, the boundary $\mathcal{C}_{bdy}$ of the region in which we consider transport is taken to be x=0.)

We first consider the case E=0.3 (Fig. 5), representing relatively coarse sediment or gentle swash. On the uprush (Fig. 5a), sediment is rapidly entrained, especially in the shallow water immediately behind the shoreline. As the flow decelerates, material is gradually deposited, so as flow reverses, at first at x=0 and then further inland, the suspended sediment concentration almost vanishes. On the backwash (Fig. 5b), concentration adjusts rapidly in the very shallow water to its instantaneous equilibrium value, and increases rapidly as the water drains offshore, carrying sediment out of the swash zone.

Essentially the same pattern occurs for E=0.01 (Fig. 6), but in this case, the greater response time of the suspended sediment load means that less material is entrained on the uprush, and concentrations well behind the shoreline remain generally lower even on the backwash. Additionally, the concentration c=c_{eq} at the shoreline decreases more rapidly as the shoreline speed falls than does that immediately behind it, forming the local maximum of c which is particularly evident in Fig. 6a.

Figs. 7b and 8b illustrate the net movement of sediment which results. In each case, there is a net landwards motion of sediment in the middle of the swash zone and a strong offshore flux seaward of this. (It is interesting to note that similar flux divergence within the swash zone has been reported by Miles et al., 2002.) The net deposit, $\eta(x)$=−dQ/dx, is positive in the upper part of the swash zone, but the dominant effect of the swash event is the erosional region in the

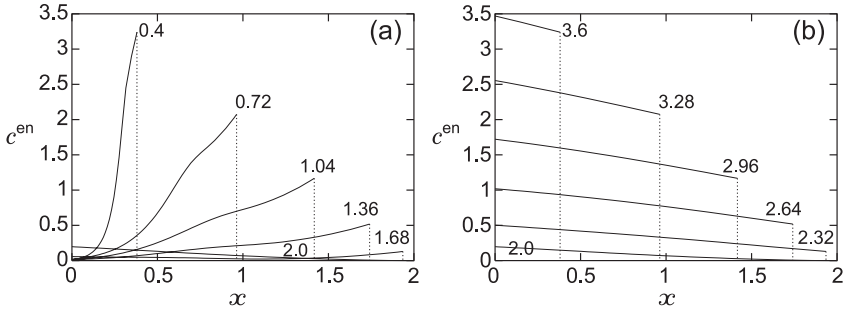

Fig. 5. Non-dimensional concentration fields $c^{\mathrm{en}}(x, t)$ plotted at regular intervals in t: (a) t=0.4 to 2 (shoreline advancing); (b) t=2 to 3.6 (shoreline retreating). Parameters throughout are E=0.3 and q_{e}=u^2; boundary condition c=0 imposed at x=0. Labels indicate the value of t for each 'snapshot' of the concentration field, and the fine dotted lines indicate the instantaneous shoreline position for each value of t.

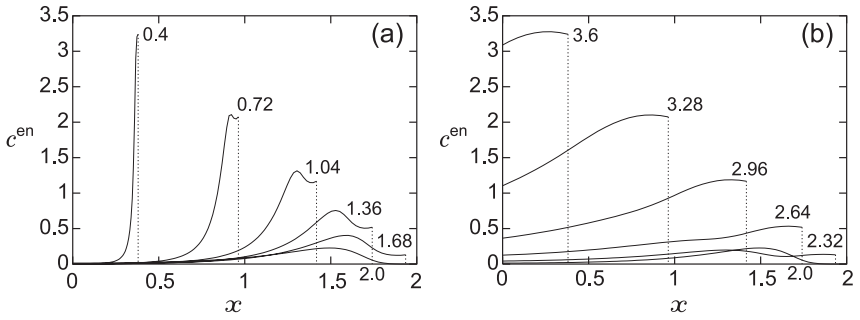

Fig. 6. Concentration fields $c^{en}(x, t)$ plotted at regular intervals in t: (a) t=0.4 to 2 (shoreline advancing); (b) t=2 to 3.6 (shoreline retreating). Parameters throughout are E=0.01 and $q_e=u^2$; boundary condition c=0 imposed at x=0. Labels indicate the value of t for each 'snapshot' of the concentration field, and the fine dotted lines indicate the instantaneous shoreline position for each value of t.

lower part, as sediment is entrained and exported on the backwash.

The net landwards transport in the upper part of the swash zone occurs through settling lag (Pritchard and Hogg, 2003a): material is entrained early in the uprush (witness the high concentrations in Figs. 5a and 6a) and gradually deposited as velocities fall towards t=2; on the backwash, it takes a finite time for high concentrations to re-establish themselves, and so on the upper part of the swash zone the seaward fluxes cannot cancel the landward fluxes. (This delay is the principal difference between the processes operating in Figs. 2a and 7b: note the effect both on the position of maximum flux during the uprush and on the magnitude of backwash fluxes generally.) The effect of a lower value of E is to shift the depositional region landwards, as it takes longer for material to be entrained on the uprush. This is also evident in the Eulerian fluxes plotted in Figs. 7a and 8a, where the peak fluxes occur earlier in both uprush and backwash for E=0.3 than for E=0.01. The generally lower concentrations for E=0.01 lead to a generally smaller net movement of sediment; the overall ratio of peak onshore to peak offshore transport, however, remains roughly the same.

4.3. Examples of solutions for pre-suspended sediment

We now consider the fate of sediment which is mobilised by the initial bore and advected into the swash zone. Figs. 9 and 10 illustrate the patterns of suspended sediment transport for high and low values of E.

In each case, the pattern of transport is fairly simple: concentrations decrease shoreward at any instant, and in a Lagrangian frame, they decrease also with time (though this is not true in an Eulerian frame because of the shorewards advection of high concentrations on the uprush: for example, an observer at x=1.2 in Fig. 9b will see first a rapid increase in c

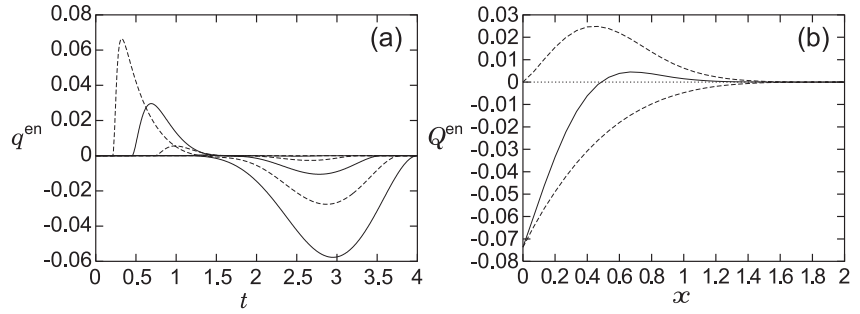

Fig. 7. (a) Non-dimensional instantaneous fluxes $q^{en}(x, t)$ at various points across the swash zone and (b) net flux $Q^{en}(x)$ over a swash event, for $q_e=u^2$, E=0.3 and boundary condition c=0 at x=0. In (a), the dashed and solid lines are for visual convenience. In (b), the dashed lines represent net fluxes on the uprush and on the backwash, while the solid line is the total flux.

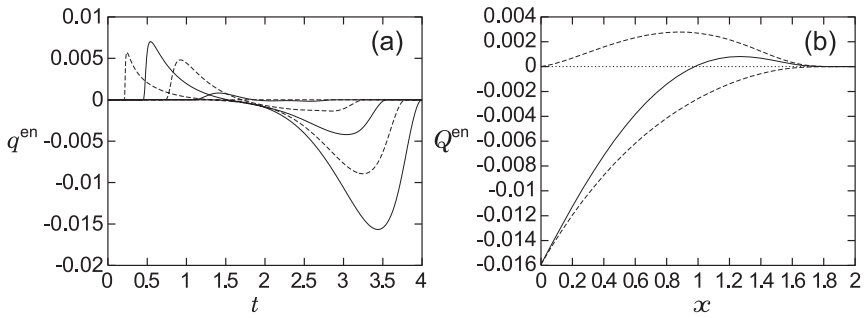

Fig. 8. (a) Non-dimensional instantaneous fluxes $q^{en}(x, t)$ at various points across the swash zone and (b) net flux $Q^{en}(x)$ over a swash event, for $q_e=u^2$, $E=0.01$ and boundary condition $c=0$ at $x=0$. In (a), the dashed and solid lines are for visual convenience. In (b), the dashed lines represent net fluxes on the uprush and on the backwash, while the solid line is the total flux.

following inundation and then a gradual decrease). The resulting pattern of net transport is entirely landwards and hence depositional; lower values of E enable sediment to be transported rather further onshore, but because there is less chance for material to settle out on the uprush, the net transport onshore is rather lower than for higher values of E, and indeed emerges only after the near cancellation of on- and offshore fluxes (Fig. 10b).

We also note that these results were obtained assuming that c takes a constant value at the seaward boundary during periods of inflow. This assumption is not necessary to our solutions, and indeed any variation of c along the boundary curve $\mathcal{C}_{bdy}$ may be imposed. However, a time-varying concentration makes little difference to the spatial pattern of deposition, since each fluid element must contribute a net flux of sediment which decays landwards regardless of its initial sediment load.

4.4. Variation of transport patterns with E and with q_e

Fig. 11 illustrates how the net sediment transport under a swash event varies with the exchange rate parameter E and with the form of the erosion rate. The net fluxes at $x=0$ of internally mobilised and externally supplied sediment (Fig. 11a and b) provide a useful measure of the overall magnitude of sediment transport in each case, although given that $x=0$ must be affected by the bore collapse they are not directly significant in themselves. The maximum landwards flux of internally mobilised sediment (Fig. 11c) provides a measure of the extent to which lag effects affect the transport processes.

Figs. 11a and b illustrate two main points. The first is that the overall trends in sediment transport under a swash event depend neither on the precise form of the erosion rate nor on whether the boundary condition is applied at $x=0$ or at $x=x_{val}(t)$; this gives us some

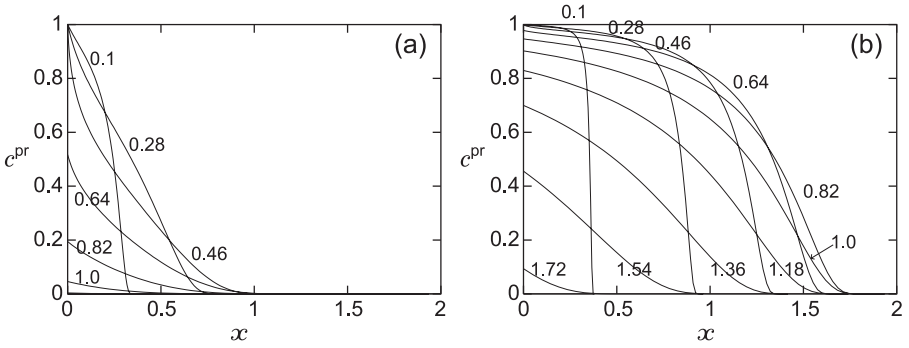

Fig. 9. Non-dimensional concentration fields $c^{pr}(x, t)$ plotted at regular intervals in t: (a) $E=0.3$; (b) $E=0.01$. Erosion rate $q_e=u^2$; boundary condition $c=1$ imposed at $x=0$. Labels indicate the value of t for each 'snapshot' of the concentration field, and the fine dotted lines indicate the instantaneous shoreline position for each value of t.

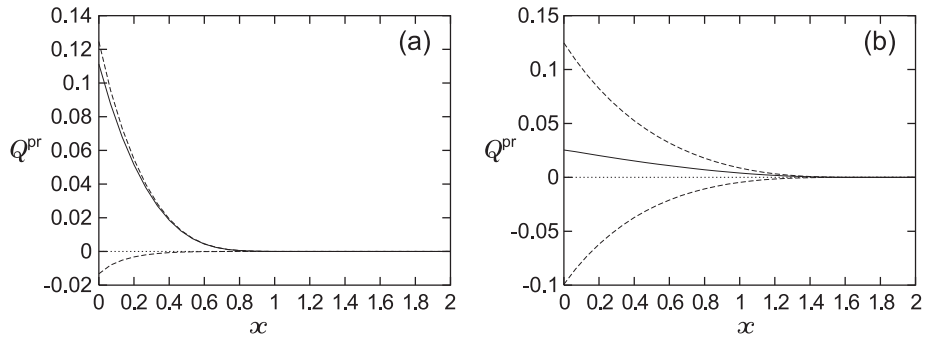

Fig. 10. Non-dimensional net fluxes $Q^{pr}(x)$ for (a) E=0.3 and (b) E=0.01. Erosion rate $q_e=u^2$; boundary condition c=1 imposed at x=0. Dashed lines represent net fluxes on the uprush and on the backwash, while the solid line is the total flux.

confidence that the results obtained here are robust. The second is that higher values of E make the swash zone both more effective in trapping sediment mobilised by the bore collapse (because it settles out more rapidly) and more able to export sediment (because of the greater amount of sediment entrained on the backwash).

Fig. 11c also illustrates two important points. For all six combinations of boundary condition and erosion rate considered, a value of $E \approx 0.1$ maximises the lag effect. However, this effect is always weak, and the maximum value of $Q^{en}(x)$ is no more than 10% of the value of $Q^{pr}(0)$. Recalling that $Q^{pr}(x)$ is calculated assuming a dimensionless boundary concentration c_0=1, this indicates that if the suspended sediment concentrations mobilised by the bore are comparable to those mobilised within the swash zone, then the principal contribution of suspended load to

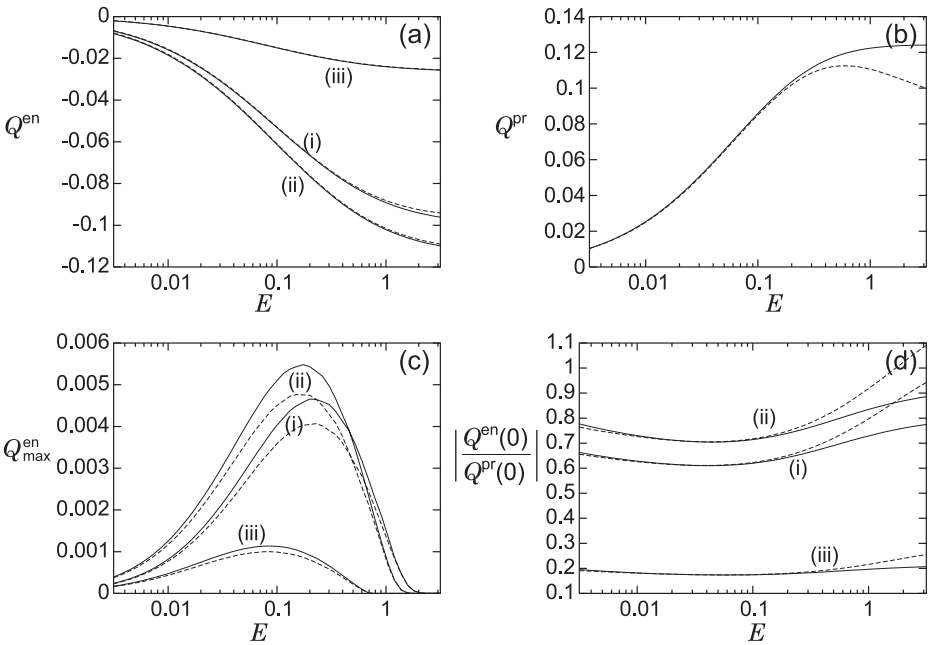

Fig. 11. Summary of variation of net transport with E and with $q_e(u)$: (a) net flux $Q^{en}(0)$ of sediment entrained in the swash zone; (b) net flux $Q^{pr}(0)$ of sediment supplied by the bore; (c) maximum positive value of $Q^{en}(x)$; (d) ratio $|Q^{en}(0)/Q^{pr}(0)|$. Solid lines represent results with boundary condition at x=0; dashed lines represent results with boundary condition at $x=x_{val}(t)$. Different forms of erosion rate: (i) $q_e=u^2$; (ii) $q_e=u^3$; (iii) $q_e=u^2-1$ when $|u|>1$.

onshore sediment transport will almost invariably be by importing sediment from the bore collapse region rather than through 'internal' lag effects.

The existence of a value of E which maximises the lag effect, and thus of weak sediment sorting across the swash zone, is a rather robust feature of our model. At low values of E, however, the lag effect must decline since $Q(x)$ becomes proportional to E in this regime (Eqs. (29) and (30)). In the opposite limit $E\rightarrow\infty$, we show in Section A.2 that for sufficiently large E, the net flux near x=2 must become negative, implying that lag effects are unable to overcome the tendency to export sediment. This explains why $Q^{\mathrm{en}}(x)$ no longer has a local maximum for large E (Fig. 11c).

The ratio $|Q^{\mathrm{en}}(0)/Q^{\mathrm{pr}}(0)|$ (Fig. 11d), which represents the balance between the sediment imported and that exported, is of order 1, and it varies only by about 20% over the range of E considered. This result provides a useful guideline for future investigations of the bore collapse process, since if the bore collapse mobilises a suspended sediment concentration greater than $c_0^{\mathrm{eqm}}=|Q^{\mathrm{en}}(0)/Q^{\mathrm{pr}}(0)|$ this will result in the net import of sediment, whereas if it mobilises less sediment than this the swash event will export sediment. However, even if the sediment imported balances that exported, the different spatial patterns of erosion and deposition (Figs. 7, 8 and 10) mean that sediment will still be redistributed within the swash zone, so the swash event will still have some morphological impact. We also note that although c_0^{eqm} varies only weakly with E, it varies substantially with the form of q_{e} (in particular with the presence or absence of a threshold shear stress for sediment entrainment), suggesting that the sensitivity of model predictions to this component should always be carefully tested.

The fact that the ratio c_0^{eqm} varies so weakly with E is also interesting because of its implications for the fate of very fine material. It is tempting to suspect that suspended transport could preferentially remove fine material from beaches, because particles entrained on the uprush are unable to settle out during the backwash and are carried seawards. However, this will lead to a net export of fine material only if the concentrations of fine sediment supplied by the bore are smaller than c_0^{eqm}, and this condition does not depend strongly on the size of the sediment. This implies that, while swash may play a part in sifting fine material out of a steep beach, it alone cannot explain the absence of fine materials, and some preferential export of fine material in the inner surf zone is also required.

4.4.1. Dimensional estimates of erosion and accretion rates

So far, we have treated the sediment transport processes under a swash event in purely nondimensional terms. This provides insight into the essential dynamics of the suspended sediment; however, in order to relate the results directly to the field, it is useful to make some calculations of the magnitude of the sediment fluxes involved.

We will take the dimensional scales specified in Section 2.1.1, with $\tan\theta$=0.1 and $(\hat{g}\hat{A})^{1/2}$=1 m s^{-1}. We will use the data of Puleo et al. (2003) as a guide to the frequency of significant swash events and the concentrations attained under them: Puleo et al. found that concentrations of 100 kg m^{-3} were attained throughout the water column approximately 10 times in 4 min, so we will take for reference a depth-averaged concentration of $\hat{C}$=100 kg m^{-3}. This gives us the convenient relation that a dimensionless flux Q=1 corresponds to a dimensional flux of 10 kg m^{-1} per swash event. So, taking a quadratic erosion law, we find that for very fine sand or silt (so $\hat{w}_{\mathrm{s}}=10^{-3}$ m s^{-1} and thus $E=10^{-2}$), one swash event can export up to 200 g of suspended sediment per metre in the longshore direction (Fig. 11a). Coarser sand, for which $\hat{w}_{\mathrm{s}}=10^{-2}$ m s^{-1} and thus E=0.1, may be exported three or four times faster. On the other hand, if the initial bore mobilises concentrations greater than about $0.7\hat{C}$ (i.e., 70 kg m^{-3}; see Fig. 11d), then comparable or greater quantities are likely to be imported (Fig. 11b). Meanwhile, Fig. 11c suggests that the swash event will move amounts of the order of 10 g m^{-1} of fine or coarse sediment, or up to about 50 g m^{-1} of intermediate sediment, onshore through settling lag.

Fig. 12 shows the predicted morphological change extrapolated over 1 h (150 swash events): it illustrates how the morphological effect of the swash varies both across the swash zone and with the amount of sediment mobilised by the bore. The results for c_0=0 (where the initial bore is empty of sediment) and for c_0=1.25 (where the initial bore is heavily overloaded

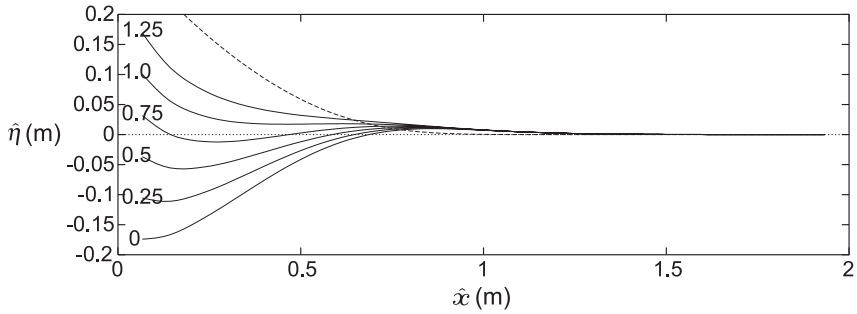

Fig. 12. Depth of net erosion or deposition under swash flow with E=0.3, $\hat{A}$=0.1 m, sinθ=0.1, $\hat{C}$=100 kg m^{-3} and $\hat{c}_b$=1800 kg m^{-3}. The dashed line represents $\hat{\eta}^{pr}(\hat{x})$; the solid lines represent $\hat{\eta}^{en}(\hat{x})+c_0\hat{\eta}^{pr}(\hat{x})$ for c_0=0, 0.25, 0.5, 0.75 and 1.25 (as labelled).

with sediment) provide an indication of the maximum erosive potential. This is greatest close to the point of bore collapse, where predicted changes are up to 15 cm per hour: we recall from Fig. 1b that shallow-water theory may not be valid seawards of $\hat{x} \approx 0.2$ m. When the bore mobilises concentrations closer to $c_0^{eqm} \approx 0.7$, the predicted morphological changes are rather lower, of the order of a few centimetres per hour.

It is worth commenting on the spatial pattern of morphological change predicted. The region close to the point of bore collapse is the most active, and also the most sensitive to the amount of pre-suspended sediment. Further landwards, the morphological change is smaller but also more independent of pre-suspension; in particular, the predicted deposition of 1–2 cm around $\hat{x}$=1 m (half way up the swash zone) is due largely to settling lag effects on sediment entrained within the swash zone, and is almost independent of c_0. When c_0 is close to c_0^{eqm}, the overall pattern of erosion and deposition may be quite complicated: for example, for c_0=0.75, there is net deposition close to the point of bore collapse, net erosion further landwards, then net deposition tailing of towards the top of the swash zone.

The morphological change predicted by naively extrapolating the results for a single swash event in this way is rather large. There are few direct measurements of the morphological change resulting from swash zone processes, but our estimate of change in the middle of the swash zone is somewhat higher than either the approximately 1 cm of deposition which Hughes et al. (1997) measured over a 4-h interval on a steep beach or the change in bed elevation of 1 cm which Butt and Russell (1999) recorded at their experimental rig over the 48-h interval between their 'calm' and 'storm' time series. (However, it is rather less than the 1 cm per swash event estimated by Puleo et al., 2003.) This discrepancy may have several causes. One is that suspended transport is only one of a number of processes occurring in the swash zone, and it may be counter-balanced by, for example, a net export of sediment in the form of bedload. A second is that changes to bed elevation of a centimetre or more are sufficient to affect the propagation of the flow itself, and so in this very dynamic environment there may be morphodynamic feedback even over a timescale of tens of minutes which prevents large features from developing. A third is that our results are exaggerated by assuming that bores always collapse in the same position and have the same size: allowing for some variation in the location and scale of swash events would mean that the sediment involved was distributed over a wider area than our naive estimates represent. However, while these discrepancies suggest that actual morphological change emerges as a rather subtle balance between different mechanisms and morphodynamic feedbacks, their overall implication is that suspended load contributes significantly to this balance.

We should now comment on the effect of allowing for the vertical distribution of sediment in the water column. As indicated in Section 2, this should probably be regarded as a source of uncertainty in the model, since it arises from processes which are hard to measure in the field or to represent accurately in models. Increasing the effective settling velocity by a factor of 10 would mean that the value of E for fine to medium sand could be as high as $E \approx 1$: referring to Fig. 11, this could increase the dimensionless net

fluxes in and out of the swash zone by up to 50%, but without much altering the ratio between them. The contribution from settling lag, however, would be almost entirely eliminated (Fig. 11c), so reducing the amount of deposition around x=1.

Finally, we note that these estimates assume that transport processes can be characterised by a single representative size of swash event. In reality, the swash will be non-uniform, and transport will be dominated by less frequent but larger events. In this case, whether the long-term erosion or accretion rates are lower or higher than those estimated here will depend on the extent to which the lower frequency of large events is offset by the ability of the larger collapsing bore to mobilise higher suspended sediment concentrations. This is clearly a complicated topic requiring further detailed field and laboratory investigation to characterise not just individual events but a representative ensemble of swash sizes and pre-suspended sediment concentrations.

5. Discussion: onshore or offshore transport?

The ultimate reason for studying sediment transport under swash is that it may be important in determining the morphodynamic evolution of beaches, with implications especially for coastal defence. In this context, the simplest question which should be answered is whether swash flows tend to move sediment seawards or landwards across the swash zone.

Although the intrinsic asymmetry between uprush and backwash velocities tends to encourage the export of sediment, we have seen that swash events may lead to landward transport through two mechanisms. Firstly, they may be effective in distributing across the swash zone all or some of the sediment mobilised by bore collapse; secondly, settling lag effects may promote a weak onshore movement of sediment. For fine sediment, the sediment load is significantly different from that predicted by a quasi-steady 'total load' model because of lag effects, whereas for relatively coarse sediment, settling lag is less effective. However, settling lag is a weak effect compared both to the onshore transport of pre-suspended sediment and to the offshore transport caused by high backwash velocities, both of which are more effective for coarser sediment. This has implications for the development of more sophisticated models for engineering applications, because it implies that these models should incorporate some description of the pre-suspension process in order to provide realistic results. (The recent experiments of Kobayashi and Lawrence, 2004 with solitary waves have suggested that this is a complex topic, as the amount of presuspended sediment depends on the manner in which the incoming wave plunges or collapses as it approaches the shoreline.)

It is interesting to consider our results in the light of recent field studies of sediment transport in the swash zone. As noted in Section 2.2, the intrinsic asymmetry in swash flows might be expected to encourage the seaward movement of sediment. However, measurements of sediment transport in the swash zone (e.g., Masselink and Hughes, 1998; Butt and Russell, 2000) have suggested that rather higher concentrations are associated with the uprush than with the backwash, so that a swash event may in fact lead to the upshore movement of sediment. A number of explanations for this phenomenon have been advanced in recent years. Several recent studies (Masselink and Hughes, 1998; Nielsen, 2002; Jackson et al., 2004) have pointed to the importance of the onshore advection of sediment mobilised by the bore collapse, but hitherto this mechanism has proved rather hard to investigate quantitatively. The results of Section 4, and in particular the estimate which they provide of the quantity of sediment which must be presuspended in order to produce a net onshore sediment flux, provide a basis against which future field measurements in both the swash and surf zone could be compared. Given the complexity of the bore collapse process such future studies are essential if the morphodynamic role of suspended sediment in the swash zone is to be properly understood; however, the dimensional estimates obtained in Section 4.4.1 suggest that the onshore advection of pre-suspended sediment may contribute significantly to net transport patterns.

It is worth setting this conclusion alongside two other theories which have recently been advanced to explain the onshore transport of sediment: a bias introduced by directionally dependent bed shear stresses, and a bias introduced by contributions

made by acceleration to the effective bed shear stress.

Masselink and Hughes (1998) found that the observed trends in uprush and backwash transport could be explained using the energetics-based model of Bagnold (1966) if different coefficients of proportionality were employed during the two phases of the flow, and suggested that this might be due to the different structure of the turbulent boundary layer or to sediment stabilisation or destabilisation by flow through the porous bed. This theory has recently received support from the direct measurements of stress carried out by Conley and Griffin (2004), and we have examined it in Section 3.1. Our tentative conclusion is that while this effect may contribute to net onshore sediment transport, it cannot lead to onshore transport everywhere in the swash zone unless c_D is taken to be rather lower on the backwash than Conley and Griffin's results suggest. It may, however, complement the onshore contribution from presuspended sediment, particularly in the upper part of the swash zone where the flow is more nearly symmetrical between uprush and backwash, whereas pre-suspended material is deposited mostly in the lower part of the swash zone. A more detailed examination of the interaction between these processes is beyond the scope of the current study, though it would make an interesting topic for future research.

Nielsen (2002) suggested that the effective shear stress exerted on the bed includes a contribution from the horizontal pressure gradient (equivalently, from the local fluid acceleration). Such a mechanism was revealed to operate in sheet flow by the particle-based simulations of Drake and Calantoni (2001), and Nielsen's (2002) analysis of Masselink and Hughes's (1998) data suggested that it could indeed explain the net transport patterns which they found, although Nielsen noted that the existing evidence is insufficient to explain the phenomenon conclusively. Recently, Puleo et al. (2003) have carried out a similar analysis of another data set, again with promising results.

We could in principle incorporate an accelerative contribution to shear stress in the analysis presented here, and this might also make an interesting topic for further numerical or analytical investigation. However, we note that there are differences between the typical records of velocity and acceleration predicted by the Shen–Meyer solution and those measured by Masselink and Hughes (1998). In particular, Masselink and Hughes (1998) measured velocities in very shallow water which increased rapidly just after inundation and decreased rapidly just before denudation: The associated high landwards accelerations play an important role in Nielsen's (2002) analysis. These accelerations, however, are absent in the Shen–Meyer solution (Fig. 13a) and in more complex simulations of swash flow; Hughes and Baldock (2004) have suggested that their appearance in some field data may be an artefact, related to the difficulty of measuring velocities accurately in very shallow water. In any case, as indicated in Section 3, it is not clear that a model in which significant transport takes place in very shallow water is physically consistent. Brief periods of high shorewards acceleration are predicted by the Shen–Meyer solution on the lower part of the swash zone as the bore collapses (Fig. 13b), but as explained above, these correspond to the region

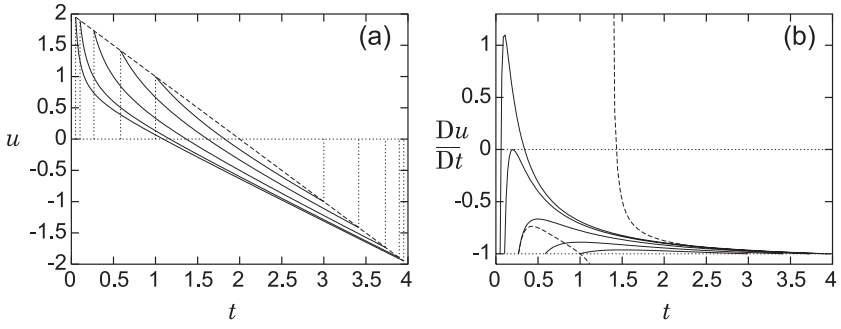

Fig. 13. Important features of Shen and Meyer's swash solution (in nondimensional variables): Eulerian measurements of: (a) velocity $u(t; x)$ (solid lines) together with shoreline velocity $2-t$ (dashed line); (b) convective acceleration $Du/Dt(t; x)$ (solid lines) plotted at x=0.1, 0.2, 0.5, 1, 1.5, together with Puleo et al.'s (2003) time series estimate $u^{-1}\partial h/\partial t-1$ (dashed line) for the point x=0.5.

$x<x_{\mathrm{val}}(t)$ in which the shallow-water description may no longer be expected to be valid.

A further difficulty involved in field studies is indicated in Fig. 13b, where we have plotted for illustration the estimate of $\mathrm{D}u/\mathrm{D}t$ derived and used in their time series analysis by Puleo et al. (2003). This estimate was derived on the basis of Taylor's hypothesis, and is given by $\mathrm{D}u/\mathrm{D}t \approx u^{-1}\partial h/\partial t - 1$. The poor correspondence between the estimate and the analytical solution indicates the difficulties faced in estimating essentially Lagrangian quantities from Eulerian time series data in the swash zone, both because the advective term $u\partial u/\partial x$ in the momentum equation cannot be neglected and because the substitution of u for the wave celerity $c = \sqrt{h}$ breaks down when the flow reverses.

The difficulties in identifying and describing complex effects such as acceleration-dependent transport clearly should not deter their further investigation, especially in the light of the discrepancies between the theoretical and empirical understanding of the flows and transport processes involved. However, our model suggests that it would be valuable to supplement such studies with systematic measurements of the amount of sediment suspended immediately offshore from the swash zone. The results presented here then provide a basis for determining the relative magnitudes of the contributions to net transport from pre-suspended sediment and that mobilised, by whatever process, within the swash zone: They support the suggestion of recent studies (Masselink and Hughes, 1998; Nielsen, 2002; Jackson et al., 2004) that the latter contribution may be significant.

6. Summary and conclusions

We have developed an analytical description of the transport of suspended sediment by a single swash event following the collapse of a bore on a plane beach, modelling the swash flow by the exact solution to the shallow-water equations obtained by Shen and Meyer (1963). We have shown how the sediment transport may be separated into a contribution from sediment entrained within the swash zone and one from sediment suspended by the initial bore collapse.

Although the intrinsic asymmetry between uprush and backwash velocities tends to encourage the export of sediment, we find that swash events may lead to landward transport. A weak settling lag effect provides part of this transport, but it is likely to be dominated by the onshore advection and settling of the sediment 'pre-suspended' by the bore collapse. For fine sediment, the sediment load is significantly different from that predicted by a quasi-steady 'total load' model because of lag effects, whereas for relatively coarse sediment, settling lag is less effective. Both the onshore transport of pre-suspended sediment and the offshore transport caused by high backwash velocities are more effective for coarser sediment. We have estimated the erosion and accretion rates which may result from suspended sediment transport, and our estimates suggest that, especially on the lower part of the swash zone, it may be as significant a mechanism as several other processes by which it has been suggested that bedload transport is biased in the landwards direction.

The calculations in this paper have been made using relatively simple flow fields and sediment transport formulae. We have demonstrated that our general conclusions are robust to variations in this formulation and we reiterate that this analytical framework may readily be employed with any flow fields and transport laws. We believe that this method offers considerable insight into the complex competing processes in nearshore morphodynamics.

The principal applicable outcome of this study is to provide an estimate of how the net erosion or deposition under a swash event is related to the quantity of sediment mobilised by the initial bore collapse. It thus provides a framework in which to address the important question identified by recent studies (Masselink and Hughes, 1998; Nielsen, 2002; Jackson et al., 2004) of how much such pre-suspended sediment may contribute to swash zone transport. Additionally, it emphasises the importance of incorporating some account of the presuspension process in future predictive models of swash zone processes. We hope that future field or experimental studies will be able to measure the pre-suspended sediment directly: with such measurements, it would be possible to build on the theoretical framework developed here and improve significantly our understanding of the important

role which the swash zone plays in nearshore morphodynamics.

Acknowledgements

DP acknowledges financial support from EPSRC and from the Newton Trust through the BP Institute. We are grateful to Dr. Gerd Masselink and an anonymous reviewer for their helpful comments on an earlier version of this paper, and to Dr. Michael Hughes for providing us with a preprint of the paper by Hughes and Baldock (2004).

Appendix A. Some asymptotic results

The following calculations provide the mathematical background to some of the general conclusions presented in the main text.

A.1. Sufficient conditions for the swash zone to export sediment under a total load model

A.1.1. Concentration-based model

We assume that sediment transport is described by a total load model in which the instantaneous concentration of suspended sediment is given by $c_{eq}(u)$. For convenience, we define the quantities $t_0(x)$ such that $u(x,\ t_0(x))=0$ and $u^*(x)\equiv u(x,\ t_{in}(x))=-u(x,\ t_{de}(x))$. The velocity at a point x then varies between u^* on the uprush and $-u^*$ on the backwash.

The total flux $Q(x)$ is given by

$$Q(x) = \int_{t_{in}(x)}^{t_{de}(x)} u(x,t)h(x,t)c_{eq}(u(x,t))\mathrm{d}t. \tag{31}$$

The flux must be zero at the top of the swash zone where $t_{in}=t_{de}$, so if we can show that $\mathrm{d}Q/\mathrm{d}x\geq 0$ throughout the swash zone, this will be sufficient to show that $Q(x)\leq 0$ throughout.

The derivative is given by

$$\frac{\mathrm{d}Q}{\mathrm{d}x} = uhc_{eq}|_{t=t_{de}}\frac{\mathrm{d}t_{de}}{\mathrm{d}x} - uhc_{eq}|_{t=t_{in}}\frac{\mathrm{d}t_{in}}{\mathrm{d}x} + \int_{t_{in}}^{t_{de}}\frac{\partial}{\partial x}\left(uhc_{eq}(u)\right)\mathrm{d}t. \tag{32}$$

By fluid continuity, we can write

$$\frac{\partial}{\partial x}\left(uhc_{eq}(u)\right) = -\frac{\partial\left(hc_{eq}\right)}{\partial t} + h\left(\frac{\partial c_{eq}}{\partial t} + u\frac{\partial c_{eq}}{\partial x}\right). \tag{33}$$

Additionally, from the definition of $t_{in}(x)$ and $t_{de}(x)$, we obtain

$$\frac{\mathrm{d}t_{in}}{\mathrm{d}x} = \frac{1}{u(x,t_{in})} \quad \text{and} \quad \frac{\mathrm{d}t_{de}}{\mathrm{d}x} = \frac{1}{u(x,t_{de})}. \tag{34}$$

Substituting these results into the expression for $\mathrm{d}Q/\mathrm{d}x$, we obtain

$$\frac{\mathrm{d}Q}{\mathrm{d}x} = \int_{t_{in}(x)}^{t_{de}(x)} h\frac{\mathrm{d}c_{eq}}{\mathrm{d}u}\left(\frac{\partial u}{\partial t} + u\frac{\partial u}{\partial x}\right)\mathrm{d}t \tag{35}$$

$$= \int_{u^*}^{-u^*} h\frac{\mathrm{d}c_{eq}}{\mathrm{d}u}(1+ug(x,u))\mathrm{d}u, \quad \text{where}$$

$$g(x,u) = \frac{\partial u/\partial x}{\partial u/\partial t} \tag{36}$$

$$= -\int_0^{u^*}\frac{\mathrm{d}c_{eq}}{\mathrm{d}u}(x,u)K(x,u)\mathrm{d}u, \tag{37}$$

where $K(x,u)\equiv h(x,u)(1+ug(x,u)) - h(x,-u)(1-ug(x,-u))$, (38)

and where in the last step we have made the additional assumption that $c_{eq}(u)$ is an even function of u.

In general, we expect $c_{eq}(u)$ to be a monotonically increasing function of $|u|$ (i.e., $\mathrm{d}c_{eq}/\mathrm{d}u\geq 0$ for $u>0$), for any physically reasonable sediment transport model. Additionally, for Shen–Meyer flow, we have

$$t(x,u) = \frac{1}{2} - \frac{3}{4}u + \sqrt{\left(\frac{1}{2} - \frac{3}{4}u\right)^2 + x} \quad \text{and}$$

$$g(x,u) = -\frac{t(x,u)}{t^2(x,u)+x}, \tag{39}$$

and it is simple to establish that $K(x,\ u)=0$ for all $(x,\ u)$ within the swash zone. This is sufficient to guarantee that $\mathrm{d}Q/\mathrm{d}x\geq 0$ and thus $Q(x)\leq 0$ across the swash zone.

A.1.2. Bailard-type model

We can carry out a similar analysis when the total load is described by a Bailard-type formula, $q=uf(u)$, where f is an even function of u. The total flux then has the form

$$Q(x) = \int_{t_{\rm in}(x)}^{t_0(x)} uf(u)\mathrm{d}t + \int_{t_0(x)}^{t_{\rm de}(x)} uf(-u)\mathrm{d}t \qquad (40)$$

and using $f(u^*)=f(-u^*)$, we may obtain

$$\frac{\mathrm{d}Q}{\mathrm{d}x} = -\int_0^{u^*} \frac{dq}{\mathrm{d}u}[g(x,u)+g(x,-u)]\mathrm{d}u, \qquad (41)$$

where $g(x, u)$ is defined as above. For any physically reasonable model, the derivative $\mathrm{d}q/\mathrm{d}u \geq 0$ for $u \geq 0$, and so the swash zone will export sediment if $g(x, u)+g(x, -u) \leq 0$ for all (x, u) in the swash zone. Again, it is simple to confirm that this is the case.

A.2. Sufficient conditions for net landwards transport at the landward end of the swash zone

It is also of interest to consider transport processes at the landwards end of the swash zone: this will give us some insight into the criteria for lag effects to produce landwards sediment transport in the upper swash zone.

We take $c_{\rm eq}(u)$ to be of the form $c_{\rm eq}=|u|^n$ where n is a positive integer. (This can be thought of as the leading term in a series expansion in small $|u|$, valid for the low velocities around maximum run-up.) As before, we express the 'total load' flux in terms of an integral over u,

$$Q_0(x) = \int_{u^*}^{-u^*} u|u|^n \frac{h(x,u)}{\partial u/\partial t}\mathrm{d}u. \qquad (42)$$

We now transform to the independent variables $\epsilon = \sqrt{2-x}$ and $v=u/\epsilon$, so this integral becomes

$$Q_0(\epsilon) = -\int_{-\sqrt{2}}^{\sqrt{2}} \epsilon^{2+n} v|v|^n f(\epsilon, v)\mathrm{d}v, \qquad (43)$$

where $f(\epsilon, v)=h/(\partial u/\partial t)$ is given by

$$f(\epsilon,v) = \frac{3}{64}\frac{\left[-12-4\epsilon v+2s-3\epsilon^2v^2+\epsilon vs+8\epsilon^2\right]^2}{12\epsilon v-2s-36-9\epsilon^2v^2+3\epsilon vs+16\epsilon^2}, \qquad (44)$$

$$\text{where} \quad s(\epsilon,v) = \sqrt{36-12\epsilon v+9\epsilon^2v^2-16\epsilon^2}. \qquad (45)$$

We now carry out an expansion in powers of ϵ, defining $f(\epsilon, v) = \sum_{n=0}^{\infty} \epsilon^n f_n(v)$. The first non-zero term is $f_4(v)$, but it turns out that the first term which we require occurs somewhat further down the series. This occurs for two reasons. Firstly, if a term $f_m(v)$ is even in v then the odd quantity $f_m(v)v|v|^n$ must integrate to zero over the symmetrical range $v = -\sqrt{2}$ to $\sqrt{2}$. Meanwhile, the structure of $f(\epsilon, v)$ means that the coefficient of any odd power of ϵ must be odd in v, and vice versa. Hence f_4, f_6 and so on cannot contribute to $Q_0(\epsilon)$, and we need only consider f_5, f_7 and so forth. Furthermore, we find that $f_5(v)=0$, and therefore the first contribution arises from $f_7(v)$:

$$f_7(v) = \frac{v}{972}\left[\frac{3}{8}v^6-\frac{7}{4}v^4+\frac{5}{2}v^2-1\right] \qquad (46)$$

and so

$$Q_0(\varepsilon) \backsim -2\epsilon^{9+n}\int_0^{\sqrt{2}} v^{1+n}f_8(v)\mathrm{d}v \quad \text{as} \quad \epsilon \to 0 \qquad (47)$$

$$= -\left(\frac{2}{3}\right)^5 \frac{2^{(n-1)/2}n}{(9+n)(7+n)(5+n)(3+n)}\epsilon^{9+n}. \qquad (48)$$

To establish whether lag effects can overcome this weak export of sediment from the upper swash zone, we need to evaluate the non-equilibrium suspended sediment concentration to some degree of accuracy. As we aim to determine the maximum value of E for which lag effects can overcome the intrinsic asymmetry and lead to onshore transport, we will use the asymptotic expansion given by Eqs. (27) and (28) which is valid for large E. Using this expansion, we can write $Q(x) \sim Q_0(x)+E^{-1}Q_1(x)+\ldots$, where

$$Q_1(x) = -\int_{t_{\rm in}(x)}^{t_{\rm de}(x)} h^2(x,t)\frac{\mathrm{D}u}{\mathrm{D}t}u\frac{\mathrm{d}c_{\rm eq}}{\mathrm{d}u}\mathrm{d}t \qquad (49)$$

$$= n\int_{-u^*}^{u^*} j(x,u)|u|^n\mathrm{d}u \quad \text{where}$$
$$j(x,u) = \frac{h^2}{\partial u/\partial t}\frac{\mathrm{D}u}{\mathrm{D}t} \qquad (50)$$

In the same way as before, we transform to the independent variables ε and v, obtaining

$$Q_1(\epsilon) = \epsilon^{1+n} \int_{-\sqrt{2}}^{\sqrt{2}} j(\epsilon, v)|v|^n \mathrm{d}v; \tag{51}$$

expanding in powers of ϵ, we find that

$$j(\epsilon, v) \sim \epsilon^8 \frac{v^8 - 8v^6 + 24v^4 - 32v^2 + 16}{20736}, \tag{52}$$

and since the leading term in the integrand is now even in v, this provides the dominant contribution to $Q_1(\epsilon)$, giving

$$Q_1(\epsilon) \sim \frac{16}{27} \frac{2^{(n+1)/2} n}{(1+n)(3+n)(5+n)(7+n)(9+n)} \epsilon^{9+n}$$

$$\text{as} \quad \epsilon \to 0. \tag{53}$$

The leading power of ϵ in the expansion of $Q_1(\epsilon)$ is the same as that in the expansion of $Q_0(\epsilon)$. This allows us to obtain a simple criterion for landward transport in the uppermost part of the swash zone: assuming that the large-E expansion is a good approximation, landward transport will occur if

$$-\left(\frac{2}{3}\right)^5 \frac{2^{(n+1)/2} n}{(9+n)(7+n)(5+n)(3+n)} + \frac{1}{E} \frac{16}{27} \frac{2^{(n+1)/2} n}{(1+n)(3+n)(5+n)(7+n)(9+n)} > 0, \tag{54}$$

i.e., if

$$E < E_0(n) \equiv \frac{9}{1+n}. \tag{55}$$

This remarkably simple result predicts, for example, that landwards net transport should not occur for $E>3$ when $n=2$, or for $E>9/4$ when $n=3$. A close inspection of Fig. 11c indicates that these predictions are reasonably accurate, although this is slightly obscured by the rapid decrease of $Q_{\max}^{\mathrm{en}}$ as E approaches $E_0(n)$.

A.2.1. Different friction coefficients on uprush and backwash

We can use the expansion of $Q_0(\epsilon)$ in powers of ϵ to understand how having a different friction coefficient on the uprush and the backwash affects the transport pattern. We can write

$$Q_0(\epsilon) = -\int_{-\sqrt{2}}^{\sqrt{2}} \epsilon^{2+n} v B^{n/2}(v)|v|^n f(\epsilon, v)\mathrm{d}v, \tag{56}$$

where B is a rescaled friction coefficient (cf. Section 3.1).

The simplest model is to take $B=1$ when $v \geq 0$ and $B=\beta<1$ when $v<0$. In this case, when we carry out the expansion we find that there is no longer perfect cancellation for the even terms in the expansion of $f(\epsilon, v)$, and we obtain a leading-order term

$$Q_0(\epsilon) \sim \frac{4}{9} \frac{2^{n/2}\left(1-\beta^{n/2}\right)}{(6+n)(4+n)(2+n)} \epsilon^{6+n}. \tag{57}$$

This means that for any $\beta<1$, there will be at least a region of (weak) shoreward transport near the top of the swash zone, and if this value is sufficiently small that it does not reverse transport at the seaward end, we must have flux divergence in the swash zone.

This result may be generalised: if we take $B \sim B_0 + B_1 v$ for $|v| \ll 1$, this again disrupts the perfect cancellation, and we find that

$$Q_0(\epsilon) = \frac{8}{9} \frac{2^{(n+1)/2} B_1}{(n+7)(n+5)(n+3)} \epsilon^{6+n}. \tag{58}$$

References

Bagnold, R.A., 1966. An approach to the sediment transport problem from general physics. In: Thorne, C.R., MacArthur, R.C., Bradley, J.B. (eds.), The Physics of Sediment Transport by Wind and Water: A Collection of Hallmark Papers by R.A. Bagnold, pp. 231–291. ASCE. (Originally published as USGS Professional Paper 422-I; reprinted 1988.)

Bailard, J.A., 1981. An energetics total load sediment transport model for a plane sloping beach. Journal of Geophysical Research 86 (C11), 10938–10954.

Baldock, T.E., Holmes, P., 1999. Simulation and prediction of swash oscillations on a steep beach. Coastal Engineering 36, 219–242.

Baldock, T.E., Tomkins, M.R., Nielsen, P., Hughes, M.G., 2004. Settling velocity of sediments at high concentrations. Coastal Engineering 51, 91–100.

Barnes, T., 1996. The generation of low-frequency water waves on beaches. PhD thesis, University of Bristol.

Butt, T., Russell, P., 1999. Suspended sediment transport mechanisms in high-energy swash. Marine Geology 161, 361–375.

Butt, T., Russell, P., 2000. Hydrodynamics and cross-shore sediment transport in the swash-zone of natural beaches: a review. Journal of Coastal Research 16 (2), 255–268.

Butt, T., Russell, P., Turner, I., 2001. The influence of swash infiltration–exfiltration on beach face sediment transport: onshore or offshore? Coastal Engineering 42, 35–52.

Carrier, G.F., Greenspan, H.P., 1958. Water waves of finite amplitude on a sloping beach. Journal of Fluid Mechanics 4, 97–109.

Conley, D.C., Griffin, J.G., 2004. Direct measurements of bed shear stress under swash in the field. Journal of Geophysical Research 109, C03050.

Conley, D.C., Inman, D.L., 1994. Ventilated oscillatory boundary layers. Journal of Fluid Mechanics 273, 261–284.

Cowen, E.A., Sou, I.M., Liu, P.L.-F., Raubenheimer, B., 2003. Particle image velocimetry measurements within a laboratory-generated swash zone. Journal of Engineering Mechanics 129 (10), 1119–1129.

Drake, T.G., Calantoni, J., 2001. Discrete particle model for sheet flow sediment transport in the nearshore. Journal of Geophysical Research 106 (C9), 19859–19868.

Elfrink, B., Baldock, T., 2002. Hydrodynamics and sediment transport in the swash zone: a review and perspectives. Coastal Engineering 45, 149–167.

Hibberd, S., Peregrine, D.H., 1979. Surf and run-up on a beach: a uniform bore. Journal of Fluid Mechanics 95, 323–345.

Hughes, M.G., Baldock, T.E., 2004. Eulerian flow velocities in the swash zone: field data and model predictions. Journal of Geophysical Research 109 (C18), C08009.

Hughes, M.G., Masselink, G., Brander, R.W., 1997. Flow velocity and sediment transport in the swash zone of a steep beach. Marine Geology 138, 91–103.

Jackson, N.L., Masselink, G., Nordstrom, K.F., 2004. The role of bore collapse and local shear stresses on the spatial distribution of sediment load in the uprush of an intermediate-state beach. Marine Geology 203, 109–118.

Jensen, A., Pedersen, G.K., Wood, D.J., 2003. An experimental study of wave run-up at a steep beach. Journal of Fluid Mechanics 486, 161–188.

Kobayashi, N., Johnson, B.D., 2001. Sand suspension, storage, advection and settling in surf and swash zones. Journal of Geophysical Research 106 (C5), 9363–9376.

Kobayashi, N., Lawrence, A.R., 2004. Cross-shore sediment transport under breaking solitary waves. Journal of Geophysical Research 109, C03047.

Longo, S., Petti, M., Losada, I.J., 2002. Turbulence in the swash and surf zones: a review. Coastal Engineering 45, 129–147.

Masselink, G., Hughes, M., 1998. Field investigation of suspended sediment transport in the swash zone. Continental Shelf Research 18, 1179–1199.

Masselink, G., Li, L., 2001. The role of swash infiltration in determining the beachface gradient: a numerical study. Marine Geology 176, 139–156.

Masselink, G., Evans, D., Hughes, M.G., Russell, P., 2004. Suspended Sediment Transport in the swash zone of a dissipative beach. (Under review).

Matsunaga, N., Honji, H., 1980. The backwash vortex. Journal of Fluid Mechanics 99, 813–815.

Miles, J.R., Butt, T., Russell, P.E., Masselink, G., Evans, D., Ganderton, P., Huntley, D.A., 2002. Swash zone sediment dynamics on steep and shallow beaches (presented at AGU Fall Meeting: see EOS Transactions 83(47), Abstract OS72C-01).

Nielsen, P., 2002. Shear stress and sediment transport calculations for swash zone modelling. Coastal Engineering 45, 53–60.

Peregrine, D.H., 1972. Equations for water waves and the approximations behind them. In: Meyer, R. (Ed.), Waves on Beaches and Resulting Sediment Transport. Academic Press, pp. 95–121. Chapter 3.

Peregrine, D.H., Williams, S.M., 2001. Swash overtopping a truncated plane beach. Journal of Fluid Mechanics 440, 391–399.

Petti, M., Longo, S., 2001. Turbulence experiments in the swash zone. Coastal Engineering 43, 1–24.

Press, W.H., Teukolsky, S.A., Vetterling, W.T., Flannery, B.P., 1992. 2nd ed. Numerical Recipies in Fortran 77. Cambridge University Press.

Pritchard, D., Hogg, A.J., 2002. On the transport of fine sediment under dam-break flow. Journal of Fluid Mechanics 473, 265–274.

Pritchard, D., Hogg, A.J., 2003a. Cross-shore sediment transport and the equilibrium morphology of mudflats under tidal currents. Journal of Geophysical Research 108 (C10), 3313.

Pritchard, D., Hogg, A.J., 2003b. Suspended sediment transport under seiches in circular and elliptical basins. Coastal Engineering 49, 43–70.

Puleo, J.A., Holland, K.T., Plant, N.G., Slinn, D.A., Hanes, D.M., 2003. Fluid acceleration effects on suspended sediment transport in the swash zone. Journal of Geophysical Research 108 (C11), 3350.

Ritter, A., 1892. Die fortpflanzung der wasserwellen. Zeitschrift des Vereines Deutscher Ingenieure 36 (33), 947–954.

Shen, M.C., Meyer, R.E., 1963. Climb of a bore on a beach: part 3. Run-up. Journal of Fluid Mechanics 16, 113–125.

Stansby, P.K., Awang, M.A.O., 1998. Response time analysis for suspended sediment transport. Journal of Hydraulic Research 36 (3), 327–338.

Stansby, P.K., Chegini, A., Barnes, T.C.D., 1998. The initial stages of dam-break flow. Journal of Fluid Mechanics 374, 407–424.

Titov, V.V., Synolakis, C.E., 1995. Modelling of breaking and nonbreaking long-wave evolution and runup using VTCS-2. Journal of Waterway, Port, Coastal, and Ocean Engineering 121 (6), 308–316.